

## Research Article

# Functional and Structural Analysis of BPSS0140-BPSS0142 ABC Transporter That Mediates Fructose Import in *Burkholderia pseudomallei*

Shu Sian How<sup>1</sup>, Su Datt Lam<sup>2</sup>, Sheila Nathan<sup>1</sup> and Sylvia Chieng<sup>1\*</sup>

<sup>1</sup>Department of Biological Sciences & Biotechnology, Faculty of Science & Technology, Universiti Kebangsaan Malaysia

<sup>2</sup>Department of Applied Physics, Faculty of Science & Technology, Universiti Kebangsaan Malaysia

\*Corresponding author: [sylvia@ukm.edu.my](mailto:sylvia@ukm.edu.my)

### ABSTRACT

ATP-binding cassette (ABC) transporters mediate bacteria uptake or export of a variety of solutes across biological membranes. Bacterial uptake of the monosaccharides is important as a source of carbohydrate building blocks that contribute to the bacteria's major structure. *Burkholderia pseudomallei* is the etiological agent of melioidosis and within its genome, 33 genes related to monosaccharide ABC transporters have been predicted. The presence of these transporters is believed to assist in bacterial survival and adaptation in various environments. Despite a large number of genes in the genome, most of these systems have yet to be characterized, including the *bpss0140-bpss0142* operon. Here, we predicted the 3D structure of each protein encoded by *bpss0140-0142* and identified the specifically associated monosaccharides. *In silico* analyses of the structures demonstrated that BPSS0140 is a sugar-binding protein, BPSS0141 is a transmembrane permease and BPSS0142 is an ATPase. Through protein structure modeling and protein-ligand docking, several specific monosaccharide sugars were found to interact with the BPSS0140-BPSS0142 ABC transporter. To validate the *in silico* prediction, knock-out mutants for each of the genes were constructed. A growth profile between wild-type and mutants in an M9 medium supplemented with glucose, fructose, ribose, and galactose as predicted from the protein-ligand docking was then performed. The growth of mutants decreased significantly compared to the wild-type bacteria when grown in M9 supplemented with fructose as the sole carbon source indicating that this transporter is potentially the main fructose transporter in *B. pseudomallei*.

**Key words:** ABC transporters, *Burkholderia pseudomallei*, protein-ligand docking, protein structure modeling

### Article History

Accepted: 28 November 2022

First version online: 26 December 2022

### Cite This Article:

How, S.S., Lam, S.D., Nathan, S. & Chieng, S. 2022. Functional and structural analysis of BPSS0140-BPSS0142 ABC transporter that mediates fructose import in *Burkholderia pseudomallei*. Malaysian Applied Biology, 51(5): 23-35. <https://doi.org/10.55230/mabjournal.v51i5.2335>

### Copyright

© 2022 Malaysian Society of Applied Biology

### INTRODUCTION

*Burkholderia pseudomallei* is a soil-dwelling Gram-negative bacillus that can survive and persist in various environments, including soil, surface groundwater, and plant-associated rhizospheres (Duangurai *et al.*, 2018). *B. pseudomallei* is also an intracellular pathogen that can invade and spread in humans and animals resulting in melioidosis that is predicted to cause up to 89,000 human deaths per year in tropical regions (Limmathurotsakul *et al.*, 2016). The adaptation and survival of *B. pseudomallei* in a broad range of niches are dependent on their ability to acquire carbon sources from the surrounding environment, especially within the nutrient-restricted host cells (Inglis & Sagripanti, 2006; Zulkefli *et al.*, 2021). These essential nutrient uptake is generally mediated by several transport proteins including the ATP binding cassette (ABC) transporter (Tanaka *et al.*, 2018; Liu *et al.*, 2020).

ABC transporters are a diverse group of transport proteins that consists of both importers and exporters, usually conserved from bacteria to humans, and function to transport various solutes across biological membranes (Lewinson & Livnat-Levanon, 2017; Ford & Beis, 2019). A bacterial ABC importer that facilitates nutrient uptake is typically composed of substrate-binding proteins (SBPs), two transmembrane

domains (TMDs), and two nucleotide-binding domains (NBDs). The extracytoplasmic SBPs serve as receptors to recognize and deliver specific substrates to the ABC system. The TMDs are the pair of integral membrane proteins that provide the passageway for the specific substrates to be imported into the bacterial cytoplasm, while NBDs are the ATPase subunits that act as a motor domain that produce energy through ATP binding and hydrolysis to ensure delivery of the specific substrate (Beis, 2015; Locher, 2016; Kolich *et al.*, 2020; Neville *et al.*, 2021).

In the genome of *B. pseudomallei*, many ABC transporter-encoding genes have been predicted. The 105 predicted functional ABC systems involve 340 genes as revealed by Harland *et al.* (2007), however, most of these systems remain poorly characterized including the ABC system *bpss0140-bpss0142*. This encoded ABC importer was predicted to play a role in the bacterial accumulation of monosaccharides (Harland *et al.*, 2007), the building blocks of carbohydrates that are well-described as a source of carbon and energy supply for bacteria (Jeckelmann & Erni, 2020). An earlier study identified that the *bpss0140-bpss0142* genes of this ABC transporter were overexpressed during *B. pseudomallei* intracellular growth and this indicated that BPSS0140-BPSS0142 probably assisted in *B. pseudomallei* host-pathogen interaction (Chieng *et al.*, 2012). To understand the mechanisms and function of BPSS0140-BPSS0142, the conserved domain and protein structures of each of the three proteins were predicted computationally in this study. The protein models were then docked with predicted monosaccharide ligands, which were glucose, fructose, galactose, and ribose, to determine the potential binding of each substrate. Transporter mutants were constructed and their growth in M9 minimal media supplemented with different carbon sources was evaluated to validate the predicted protein ligand-docking and the substrate(s) transported by the ABC system BPSS0140-BPSS0142.

## MATERIALS AND METHODS

### Computational analysis and protein structure modeling of the ABC transporter BPSS0140-BPSS0142

Initially, the nucleotide sequences of the genes *bpss0140*, *bpss0141*, and *bpss0142* encoding the *B. pseudomallei* ABC transporter were translated to their respective amino-acid sequence using ExPASy translate tools (<https://web.expasy.org/translate/>). The sequences were submitted to the InterPro database for functional analysis of the proteins and classification of proteins families and domains (<https://www.ebi.ac.uk/interpro/>) (Blum

*et al.*, 2021) and PSORTb v3.0.2 to determine the protein localization and presence of signal peptides (<https://www.psort.org/psortb/>) (Yu *et al.*, 2010). The amino acid sequences were also screened against the Protein Data Bank (PDB) to identify a potential homologous template for structure modeling. As only the amino acid sequences for BPSS0140 and BPSS0142 were aligned to potential homologous structures within PDB (<http://blast.ncbi.nlm.nih.gov/Blast.cgi>), the sequences were submitted to the AlphaFold v2.1.0 server for ab-initio structure prediction using the default settings to minimize possible bias towards the available structure in the predicted models (<https://colab.research.google.com/github/deepmind/alphafold/blob/main/notebooks/AlphaFold.ipynb#scrollTo=pc5-mbsX9PZC>). This AlphaFold Colab server uses no templates or homologous structures but refers to the Big Fantastic Database, the largest publicly available collection of protein families (Jumper *et al.*, 2021). Modeled structures were viewed and analyzed with the UCSF Chimera software available at <https://www.cgl.ucsf.edu/chimera/> (Pettersen *et al.*, 2004). The final predicted models were then assessed by Structural Analysis and Validation tool version 6 (SAVES v6.0) (<https://www.doe-mbi.ucla.edu/saves/>) that provides protein validation programs include ERRAT analysis for the calculation of protein's models quality factors where scores greater than 50 are acceptable for high-quality models (Colovos & Yeates, 1993) as well as PROCHECK program to verify the stereochemical quality of predicted model using Ramachandran plot (Laskowski *et al.*, 1996). The transmembrane helices of the predicted membrane protein BPSS0141 were predicted using the TMHMM server (<https://services.healthtech.dtu.dk/service.php?TMHMM-2.0>) (Krogh *et al.*, 2001).

### Protein-ligand docking of ABC transporter BPSS0140-BPSS0142

The predicted structures of BPSS0140-BPSS0142 were docked with selected ligands in a protein-ligand binding site prediction server, COACH-D (Yang *et al.*, 2013; Wu *et al.*, 2018) (<https://yanglab.nankai.edu.cn/COACH-D/>). COACH-D predicts the protein-ligand binding pockets and residues with five distinct methods (TM-SITE, S-SITE, COFACTOR, FINDSITE, and ConCavity). The ligands used (Fructose, CID 5984; Glucose, CID 107526; Galactose, CID 3037556; Ribose, CID 5311110) were obtained from PubChem (<https://pubchem.ncbi.nlm.nih.gov/>). Docking of the ligand at the predicted binding sites was done with the AutoDock Vina software (Trott & Olson, 2010). The docked models were visualized in the UCSF Chimera software.

### Bacteria and growth conditions

*B. pseudomallei* D286 wild type (a clinical isolate),  $\Delta bpss0140$ ,  $\Delta bpss0141$ , and  $\Delta bpss0142$  were plated on Ashdown agar and incubated at 37 °C for 48 h (Ashdown, 1979). *Escherichia coli* DH5 $\alpha$  and RHO3 strains were grown in Luria-Bertani (LB) agar or broth with appropriate antibiotics at 37 °C, (250 r.p.m. for broth cultures) overnight (López et al., 2009). For growth assay, *B. pseudomallei* wild type and mutants were grown in M9 supplemented with 0.4% glucose, fructose, galactose, or ribose, respectively, and incubated at 37 °C, 250 r.p.m. for up to 72 h (Vanaporn et al., 2017).

### Deletion gene mutant construction

In this study, three mutants,  $\Delta bpss0140$ ,  $\Delta bpss0141$ , and  $\Delta bpss0142$  were constructed according to López et al. (2009) and Wong et al. (2016) with some modifications. In brief, two appropriate fragments from upstream and downstream of the targeted genes were amplified from the genomic DNA of *B. pseudomallei* D286. Amplifications of upstream fragments were performed using primers 0140\_USF (5' CGTACGAACTCGACGCGAT 3') and 0140\_USR (5' GTCTCCGTATGGTCCGGGAT 3'), 0141\_USF (5' TACCGGATCATCAACGAGC 3') and 0141\_USR (5' GCTTTGCTTGATCTGTTGGTT 3'), 0142\_USF (5' CCCGATATGCAGCGTTCTGA 3') and 0142\_USR (5' CTCCTGATAGATCACC GCGAC 3'), whereas downstream fragments were amplified with primers pair 0140\_DSf (5' ATCCCGACCATACGGAGACGAGCCGACGCTCATCACG 3') and 0140\_DSR (5' GCGATGCACATTCATCCGAC 3'), 0141\_DSf (5' AACCAACAGATCAAGCAAAGCTACCGTCAGCACGGATCG 3') and 0141\_DSR (5' GGATTGATTTCTTCGCCTG 3'), 0142\_DSf (5' GTCGCGGTGATCTATCAGGAGCTGTCATTCACCTTCGGGTT 3') and 0142\_DSR (5' CACGATGTTGATCGACGCCT 3'). The fragments were then spliced together using gene specific upstream forward (USF) together with downstream reverse (DSR) primers. The fragments without targeted gene were cloned into the pEXKm5 plasmid and subsequently transformed into *E. coli* mobilizer strain RHO3. The recombinant plasmid harbouring the targeted fragment was then transferred into *B. pseudomallei* D286 through conjugation and homologous recombination resulting to the formation of either mutant or wild-type strain with the latter SacB counter selection using yeast extract tryptone agar with 15% sucrose. The clones were further screened by LB agar with 1000  $\mu$ g kanamycin and colony PCR. The colony PCR were performed as a single colony of  $\Delta bpss0140$ ,  $\Delta bpss0141$ , and  $\Delta bpss0142$  were resuspended in nucleus free water and boiled at 95 °C. The boiled colony was then used as a PCR template using primers pair of gene specific upstream forward and downstream reverse. Single colony of wild type *B. pseudomallei* D286 was used as positive control while nucleus

free water was used to replace boiled colony which acts as negative control.

### Growth profile in different carbon sources

A single colony of *B. pseudomallei* wild type and mutants were cultured into LB broth with 4  $\mu$ g/mL gentamicin at 37 °C, 250 r.p.m. overnight. The overnight cultures were diluted with fresh media until OD600 = 0.5 before further incubation. For growth assays in minimal media supplemented with different carbon sources, the *B. pseudomallei* wild type and mutant cultures were centrifuged and the pellets were resuspended individually in M9 supplemented with 0.4% of either glucose, fructose, galactose, or ribose. The cultures were then diluted until an OD600 = 0.5 was achieved. The cultures were then diluted 1:100 with fresh media and incubated at 37 °C, 250 r.p.m. Bacterial growth was measured at 600 nm every 2 h until growth reached the stationary phase.

## RESULTS AND DISCUSSION

### *In silico* functional and structure determination of BPSS0140, BPSS0141, and BPSS0142

In the *B. pseudomallei* genome, *bpss0140*, *bpss0141*, and *bpss0142* are located on chromosome 2. This is the smaller of the two *B. pseudomallei* chromosomes and the genes found on this chromosome mainly encode for functions required for adaptation and survival (Holden et al., 2004; Hall et al., 2019). The conserved domain predicted for BPSS0140 is a periplasmic binding domain (IPR025997) from the same family as the autoinducer 2-binding protein *LsrB* from *E. coli* (Xavier & Bassler, 2005) and *Salmonella typhimurium* (Taga et al., 2008) as well as the D-galactose or D-ribose binding periplasmic protein from *E. coli* and *S. typhimurium* (Berntsson et al., 2010; Scheepers et al., 2016). The sequences analysis indicated that BPSS0141 is a member of the ABC transporter permease domain (IPR001851), where this family usually consists of high-affinity branched-chain amino acid transporter proteins (Adams et al., 1990; Basavanna et al., 2009), monosaccharides transport system permeases (Woodson & Devine, 1994; Wagner et al., 2018) and nucleoside transporters (Martinussen et al., 2010). BPSS0142 is predicted to be an ATP-binding domain (IPR003439) associated with ATP binding and hydrolysis to provide energy for the transport of substrates (Kerr, 2002). In addition, residues 35-484 of BPSS0142 are predicted as an AAA+ ATPase domain (IPR003593) that facilitates various cellular processes such as DNA replication, recombination, repair, and transcription (Ogura & Wilkinson, 2001; Snider et al., 2008). The localization prediction tool, PSORTb v3.0.2

identified that BPSS0141 and BPSS0142 are localized in the cytoplasm with no signal peptide whereas BPSS0140 is localized at the periplasm with the presence of signal peptide noted.

The amino acid sequences search against the PDB showed no crystallographic structure available for BPSS0140, BPSS0141, and BPSS0142. As such, the protein structures were predicted using AlphaFold Colab. The predicted local distance difference test (pLDDT) scores of the protein models built were generally higher than 90, pLDDT scores are calculated through the per-residue estimate of confidence on a scale from 0 – 100 where model regions with pLDDT > 90 are expected to be regions of high accuracy. The pLDDT score of the BPSS0140 model has an average of 93. The BPSS0140 model was further validated with ERRAT, a module of SAVES v6.0 in which the ERRAT score was calculated from non-bonded interactions between different atom types, had shown the overall structural quality of the predicted BPSS0140 model as 100 indicating BSS0140 model is a significantly good quality model. The quality of BPSS0140 was further evaluated with a Ramachandran plot generated by PROCHECK which showed that 86.2% of the residues in the most favored region, 10.9% in additional allowed regions, and only 0.7% of residues existed in disallowed regions. Overall, more than 90% of the residues were found to be in favored and allowed regions, suggesting that the BPSS0140 model is acceptable. The BPSS0140 protein model was compared to the top 3 structures obtained from the PDB, which were sugar-binding transport protein from *Yersinia pestis* CO92 (PDB ID: 4RWE), ribose binding protein of *Thermoanaerobacter tengcongensis* (PDB ID: 2IOY) (Cuneo et al., 2008) and ribose binding protein *RbsB* of *Streptococcus agalactiae* (PDB ID: 7E7M). The value of root-mean-square deviation (RMSD) between corresponding atoms of two protein structures indicates the similarity of two protein structures, in which the RMSD for the two identical proteins is 0.00Å and the value increases as the two structures become more different, while the RMSD for *in silico* prediction model to PDB structure should be <2.50Å (Tsai et al., 2009). The structure of BPSS0140 is comparable to the three SBP structures with an RMSD 1.14Å (4RWE), 1.08Å (2IOY), and 1.83Å (7E7M). The three structures for the PDB and BPSS0140 model appear as a pair of similar intertwined globe-like subdomains, both assembled as an interchangeable super secondary structure composed of a central  $\beta$ -sheet flanked on either side by two helices (Berntsson et al., 2010).

The monomeric BPSS0141 model (Figure 1(b)) has an average of 88 for the pLDDT score.

The model assessment of BPSS0141 in ERRAT and PROCHECK demonstrated that the predicted model for BPSS0141 is generally a good quality model as the overall ERRAT score obtained for BPSS0141 is 98.75 and 92.6% of amino acids were in the most favored region of Ramachandran plot. As Ramachandran plot of an ideal structure is expected to have >90% of residues in most favored regions (Laskowski et al., 1993), confirming that the BPSS0141 predicted model is of high quality. The TMHMM transmembrane protein topology suggested that BPSS0141 contains 9 transmembranes (TM) helices. The folds of TMDs are diverse and not conserved like NBDs (Lewinson & Livnat-Levanon, 2017), therefore, there is a similar structure of BPSS0141 available in PDB. As BPSS0141 was predicted as a type I ABC importer, the BPSS0141 model was compared with a sugar ABC importer permease, maltose transporter MalF from *E. coli* (Khare et al., 2009). The structure of BPSS0141 was similar to other membrane proteins as the secondary structure of the predicted protein is made up of alpha helices that span the membrane (Zhou et al., 2004) and contains a signature motif conserved for ABC transporter permeases. The conserved motif EAA loop of BPSS0141 at residues 223-241 within TM6 and TM7 (predicted by InterPro), is required for its interaction with the ATP-binding subunits.

The pLDDT of model BPSS0142 (Figure 1c) has an average of 88. Besides, BPSS0142 estimated overall quality factor by ERRAT was 97.19 while Ramachandran plot qualities showed the percentage of residues in BPSS0142 that belonging to the favored (91.6%), allowed (6.8%), generally allowed (1.4%) and disallowed (0.2%) region of the plot, which indicated that the BPSS0142 chosen model was of good quality. The BPSS0142 model was compared with reported NBD structures from PDB which are 4TQV (RMSD 1.94Å), 4TQU (RMSD 2.03Å), and 4XTC (RMSD 2.08Å) from *Sphingomonas* sp. (Maruyama et al., 2015; Kaneko et al., 2017). The predicted BPSS0142 model has the ABC signature motif also known as the C loop which is the position for ATP hydrolysis in the ABC systems. BPSS0142 also exhibits several NBD conserved motifs that were identified through InterPro, such as Walker A (phosphate-binding loop), Walker B (magnesium binding site) (Kerr, 2002), Q loop (interacts with gamma phosphate of the ATP molecule through a water bond) (Thomas & Tampé, 2020), D loop (coordinates the attacking nucleophile) (Jones & George, 2012) and H loop (contain the conserved active site histidine that donates a hydrogen bond to gamma phosphate of the ATP to stabilize its position in the active site) (Linton & Higgins, 2007).

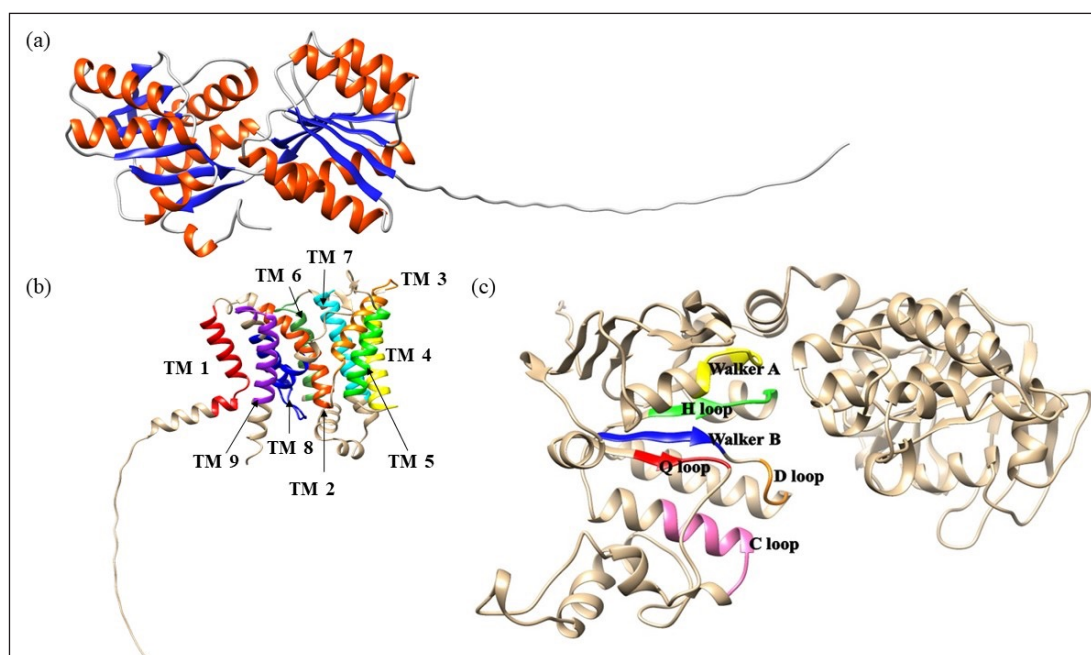


**Fig. 1.** Protein models predicted for *B. pseudomallei* (a) BPSS0140, (b) BPSS0141, (c) BPSS0142. The BPSS0141 model is colored according to its secondary structure. The TM helices of BPSS0141 identified using TMHMM are colored differently and labeled. Monomeric NBD BPSS0142 with mechanistically important sequence motifs identified from InterPro are colored and labeled as Walker A (yellow), Walker B (blue), Q loop (red), C loop, or LSGGQ motif (pink), H loop (green), and D loop (orange).

### Potential ligands and the binding site for BPSS0140, BPSS0141, and BPSS0142

BPSS0140-0142 was predicted as an ABC importer belonging to the MOS (monosaccharides) family involved in the uptake of monosaccharides such as ribose, glucose, and galactose in *B. pseudomallei* (Harland *et al.*, 2007). Potential ligands were predicted from the *in-silico* analysis and fructose, glucose, galactose, and ribose were selected to dock with the Alpha Fold predicted protein models of BPSS0140, BPSS0141, and BPSS0142. Docked models of BPSS0140 with different predicted ligands are illustrated in Figure 2 and docking results are summarised in Table 2. The more negative the binding energy, the higher the binding possibility of the substrate toward the protein model (Gaillard, 2018). BPSS0140 was predicted as an SBP from the *in silico* analysis described above and a previous study revealed that SBPs function to scavenge its ligand through high affinity and specificity binding sites and deliver the substrate to the appropriate transporter in the system for the substrate to be transported into the cell (Scheepers *et al.*, 2016). Hence, the ligand that can bind favorably with BPSS0140 is more likely to be associated with this ABC transporter. The docked models of BPSS0140 were predicted using the known protein-ligand interaction of a periplasmic solute binding protein from *Streptobacillus moniliformis* (PDB ID: 4Z0N) and its ligand D-galactose. The protein-ligand

docking data obtained for BPSS0140 suggested that galactose is the most possible substrate to bind to this SBP as well as glucose, fructose, and ribose.

BPSS0141 is the integral membrane subunit that provides the channel for substrate translocation and the predicted docked models (Figure 3) were assembled by random docking due to the lack of a protein-ligand interaction template identified from PDB. The ligand was predicted to bind at TM3 (Ala102, Ala103, Ala104), TM4 (Leu125, Ala126, Val127, Gly128) and TM7 (Leu246, Gly248). The docked model of BPSS0141 showed that the binding affinities between the protein and substrates are generally low compared to BPSS0140 and BPSS0142. The binding energy for fructose is more negative, indicating a more stable binding compared to galactose and ribose, while glucose binds less stably to BPSS0141 suggesting it is the monosaccharide less likely to bind to the predicted ABC transporter permease. BPSS0142's predicted role in the ABC system is ATP hydrolysis to supply the energy needed for translocation. The protein-ligand interaction of *Sulfolobus solfataricus* glucose transport ATPase protein (Verdon *et al.*, 2003) was referred for the BPSS0142 docked model (Figure 4). The docking results illustrated that galactose (Table 2) is one of the top 3 monosaccharides that has the highest affinity towards BPSS0142 followed by glucose and fructose.

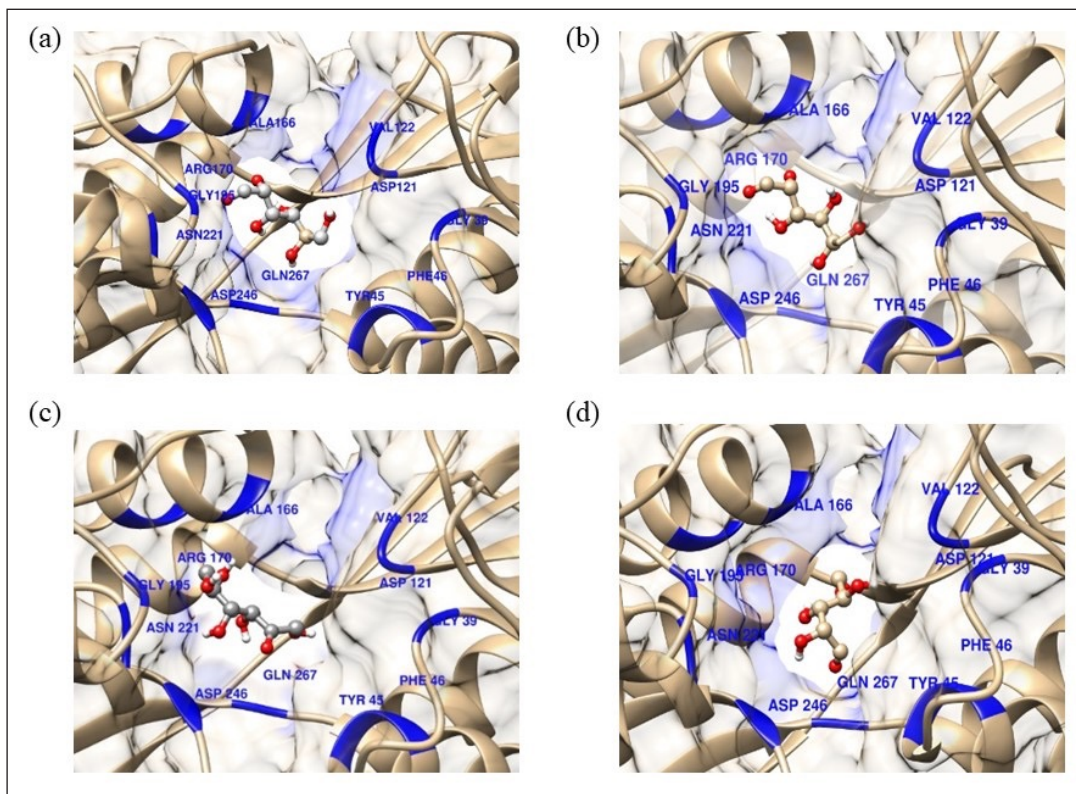


**Fig. 2.** Docked models of BPSS0140 with (a) glucose, (b) galactose, (c) fructose, and (d) ribose. The residues colored blue are the predicted residues that interact with the ligand.

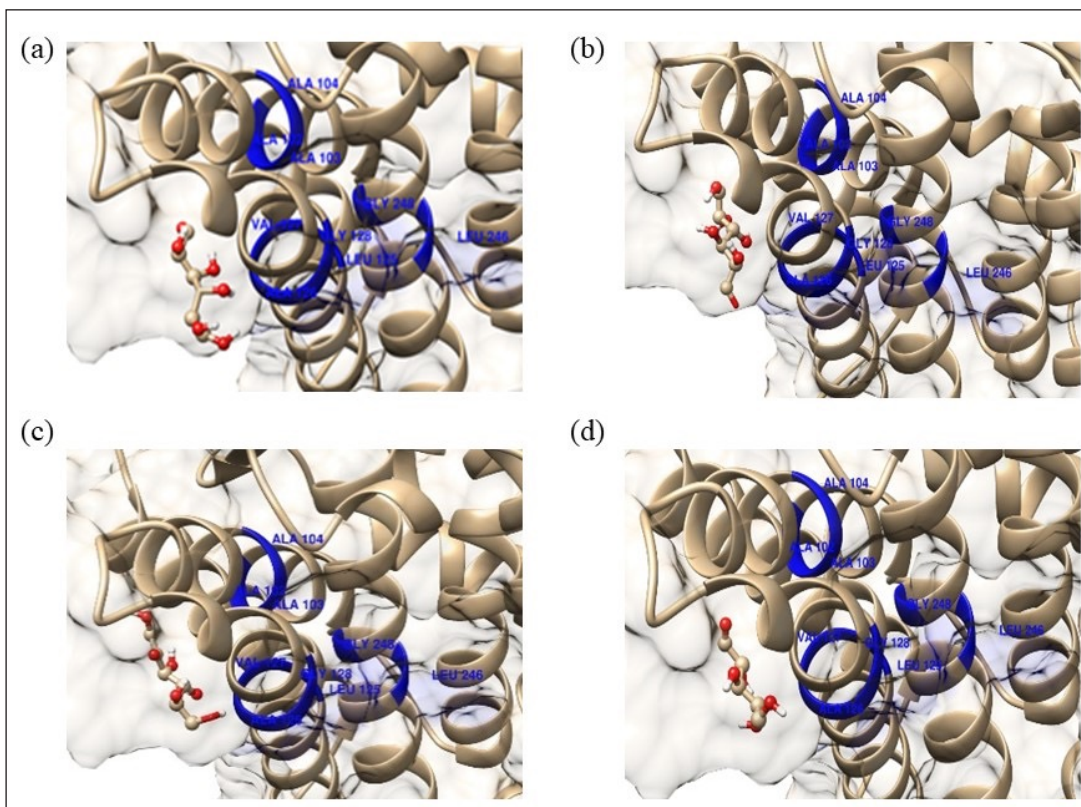


**Fig. 3.** Docked models of BPSS0141 with (a) glucose, (b) galactose, (c) fructose, and (d) ribose. The residues colored blue are the predicted residues that interact with the ligand.

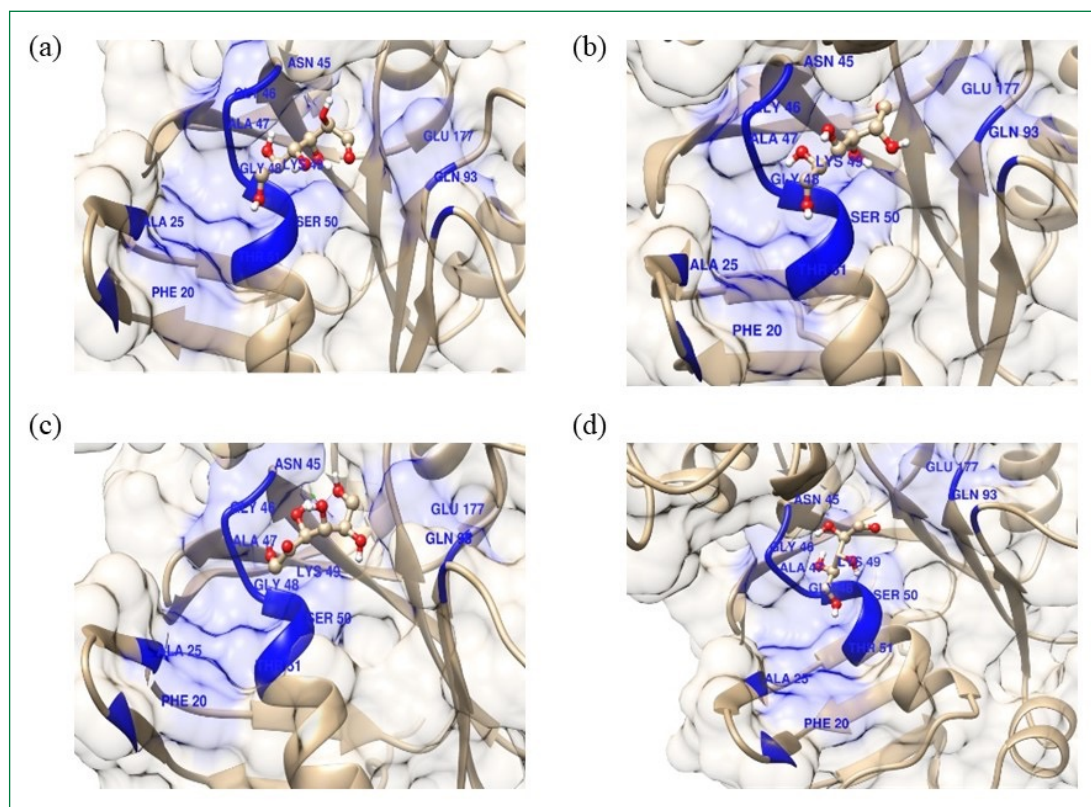


**Fig. 4.** Docked models of BPSS0142 with (a) glucose, (b) galactose, (c) fructose, and (d) ribose. The residues colored blue are the predicted residues that interact with the ligand.

**Table 1.** Functional and localization analysis of BPSS0140-BPSS0142

Protein	Conserved domain	Cellular localization	Signal peptide
BPSS0140	Periplasmic binding domain (IPR025997)	Periplasm	Detected
BPSS0141	ABC transporter permease (IPR001851)	Cytoplasm	Not detected
BPSS0142	ATP-binding domain (IPR003439) / AAA+ ATPase domain (IPR003593)	Cytoplasm	Not detected

**Table 2.** Protein-ligand simulations of BPSS0140-BPSS0142 docked to different monosaccharides

Protein Model	Interacting residues	Monosaccharides	Binding energy (kcal/mol)
BPSS0140	Gly39, Try45, Phe46, Asp121, Val122, Ala166, Arg170, Gly195, Asn221, Asp246, Gln267	Glucose	-4.6
		Galactose	-5.1
		Fructose	-4.7
		Ribose	-4.7
		Glucose	-1.9
BPSS0141	Ala102, Ala103, Ala104, Leu125, Ala126, Val127, Gly128, Leu246, Gly248	Galactose	-2.3
		Fructose	-2.6
		Ribose	-2.3
		Glucose	-4.5
BPSS0142	Phe20, Ala25, Asn45, Gly46, Ala47, Gly48, Lys49, Ser50, Thr51, Gln93, Glu177	Galactose	-4.6
		Fructose	-4.5
		Ribose	-4.1

### Construction of $\Delta bpss0140$ , $\Delta bpss0141$ , and $\Delta bpss0142$

The mutants  $\Delta bpss0140$ ,  $\Delta bpss0141$ , and  $\Delta bpss0142$  were constructed as previously described. Gel electrophoresis of colony PCR using primers pair from upstream forward and downstream reverse for respective genes illustrated differences in amplicon size for three mutants  $\Delta bpss0140$ ,  $\Delta bpss0141$ , and  $\Delta bpss0142$  as compared with wild-type *B. pseudomallei* (Figure 5). The fragments amplified from mutants demonstrated a decrease in band size in comparison to the wild type as the targeted gene is deleted from the mutant's genome. The single band observed in Well 1 for  $\Delta bpss0140$  without the targeted gene was predicted to be 564 bp, while the wild type with the targeted gene was 1458 bp, as shown in Well 2 (Figure 5). The appropriate band size for  $\Delta bpss0141$  is 573 bp while the wild type is 1554 bp which is clearly shown in Figure 5. For  $\Delta bpss0142$ , the predicted amplicon size without the targeted gene is 549 bp, while the size of the positive control with *bpss0142* intact is 1836 bp. The amplicon size of the three mutants is easily distinguishable from wild-type *B. pseudomallei* D286 validating the successful generation of  $\Delta bpss0140$ ,  $\Delta bpss0141$ , and  $\Delta bpss0142$ .

### Growth profile of $\Delta bpss0140$ , $\Delta bpss0141$ , and $\Delta bpss0142$

The growth profile of the mutants  $\Delta bpss0140$ ,  $\Delta bpss0141$ , and  $\Delta bpss0142$  compared to wild-type *B. pseudomallei* in nutrient-rich LB broth (Figure 6a) was similar suggesting that the loss of these individual genes from the *B. pseudomallei* genome did not affect bacterial growth. Similarly, the growth of the mutants in M9 minimal media supplemented with glucose (Figure 6b) and galactose (Figure 6c) was similar to wild-type *B. pseudomallei*. Although these results do not reflect the protein-ligand docking analysis, the presence of other reported sugar transporters such as the sugar phosphotransferase system (PTS) (Barabote & Saier, 2005) proposes that BPSS0140-0142 ABC transporter may not be the major transporter for galactose and glucose. Interestingly, the growth of the mutants was decreased compared to the wild type in M9 supplemented with fructose (Figure 6d) demonstrating that BPSS0140-0142 is a *B. pseudomallei* fructose ABC transporter. This outcome corresponded to the protein-ligand docking analysis for BPSS0141. The three proteins BPSS0140-0142 work together to translocate fructose as loss of either gene-restricted *B. pseudomallei* growth in M9 supplemented with fructose.

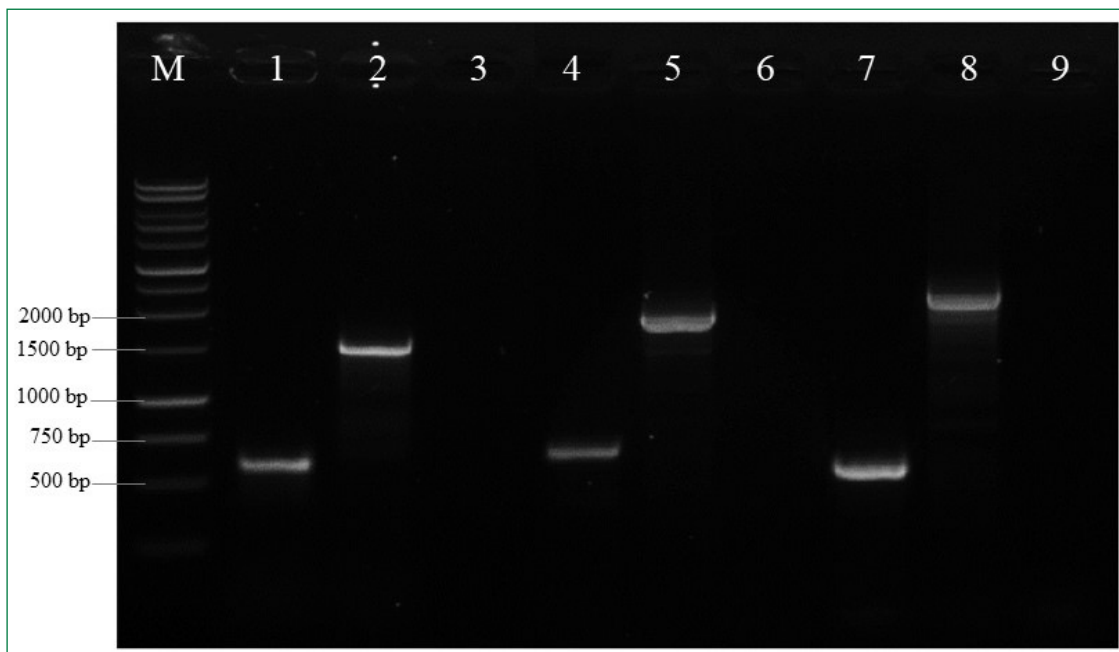


**Fig. 5.** PCR colony validation of  $\Delta bpss0140$ ,  $\Delta bpss0141$ , and  $\Delta bpss0142$  using gene-specific upstream forward and downstream reverse primers. A single colony of wild-type *B. pseudomallei* D286 was used as positive control while nucleus-free water was used to replace the boiled colony which acts as a negative control. M represents 1 kb DNA ladder (Promega, Co., Madison, WI, USA); Well 1:  $\Delta bpss0140$ ; Well 2:  $\Delta bpss0140$  positive control; Well 3:  $\Delta bpss0140$  negative control; Well 4:  $\Delta bpss0141$ ; Well 5:  $\Delta bpss0141$  positive control; Well 6:  $\Delta bpss0141$  negative control; Well 7:  $\Delta bpss0142$ ; Well 8:  $\Delta bpss0142$  positive control; Well 9:  $\Delta bpss0142$  negative control

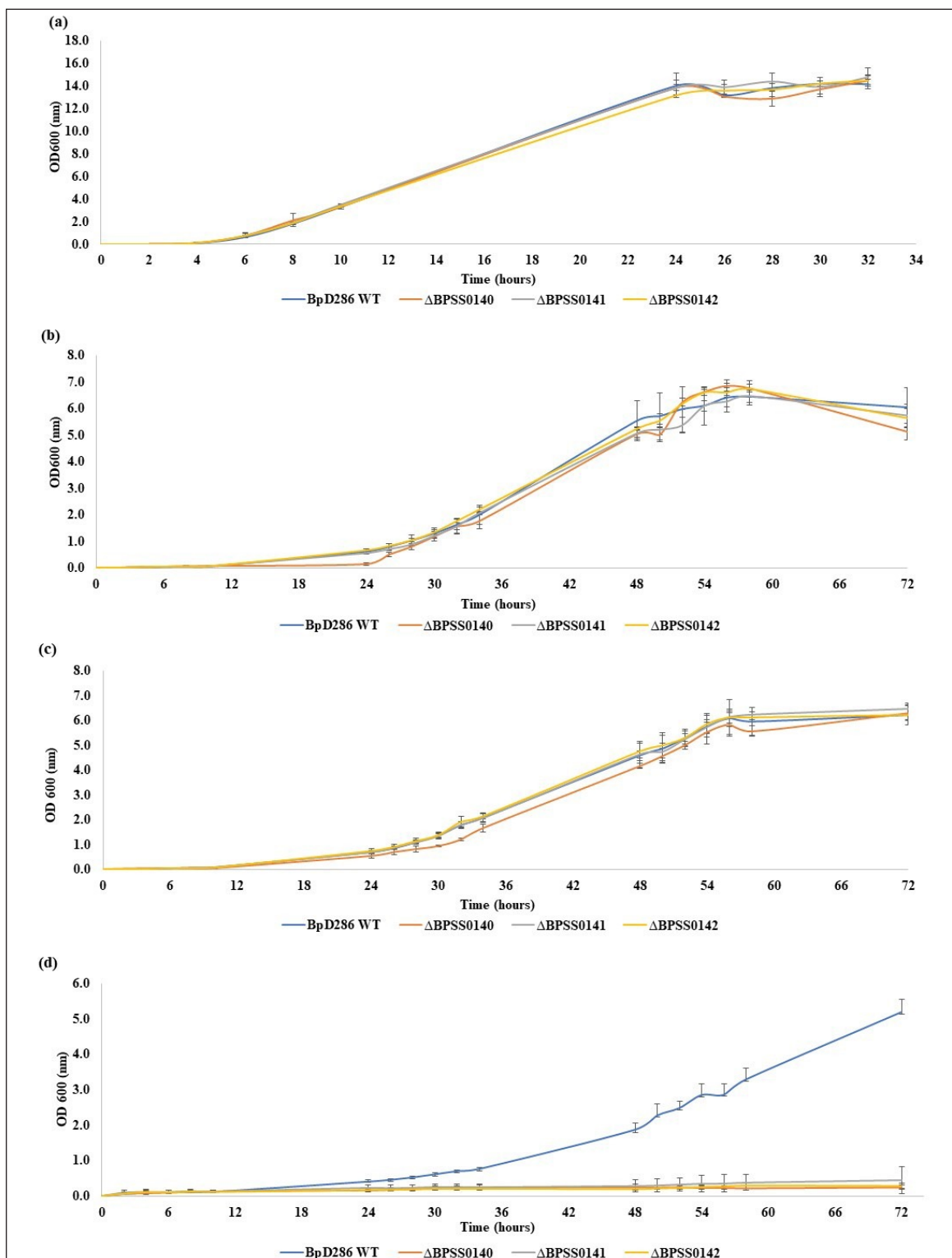


**Fig. 6.** Growth profiles of *B. pseudomallei* D286 wild type,  $\Delta$ *bpss0140*,  $\Delta$ *bpss0141*, and  $\Delta$ *bpss0142* in M9 media supplemented with different monosaccharides. (a) LB, (b) M9 + glucose, (c) M9 + galactose, (d) M9 + fructose. *B. pseudomallei* wild type and mutants grew rapidly in rich media (LB) and reached stationary phase after 24 h of incubation. Growth was relatively slow in M9 supplemented with glucose and galactose. In contrast, the growth rate of mutants in M9 + fructose is extremely low compared to the wild type and mutants in other carbon sources.

The results also show that *B. pseudomallei* fructose uptake does not rely on the major reported fructose transport system in Gram-negative bacteria which is fructose-specific PTS that performs fructose uptake through the production of fructose-1-phosphate (Wei et al., 2012). There is another fructose ABC transporter reported in the Gram-negative *Sinorhizobium meliloti* (Mandon et al., 2001), however, the available information about fructose-specific ABC system is limited for Gram-negative bacteria, especially in *B. pseudomallei*. The growth of mutants and wild type in M9 supplemented with ribose was also assessed but neither mutants nor wild type successfully grew in the ribose-supplemented media (data not shown). Strangely, the functional and structural prediction of BPSS0140-0142 exhibited significant homology to ribose transport proteins in other bacteria. In addition to *bpss0140-0142*, the ABC systems *bps1832-1834* and *bpss0255-0257* are predicted to encode for *B. pseudomallei* ribose transporters in Harland et al. (2007), however, the results in this study showed that the *B. pseudoamallei* D286 strain cannot assimilate ribose for its cellular metabolism.

## CONCLUSION

The nutrient acquisition is essential for the survival of bacteria and carbohydrates or sugars serve as crucial carbon and energy carriers for bacterial cellular metabolism. The carbohydrates

or sugar critical for bacteria survival are delivered by members of the ABC transporter family. ABC transporters are ubiquitously present in all living things and conduct miscellaneous functions (Thomas & Tampé, 2020). In the present study, we carried out an *in silico* analysis of the *B. pseudomallei* ABC transporter BPSS0140-0142 to determine the function(s) based on predicted structures. This ABC transporter is considered an importer and is mainly responsible for the translocation of fructose into *B. pseudomallei*. The loss of either gene (*bpss0140* or *bpss0141* or *bpss0142*) in ABC transporter will affect the uptake of fructose in *B. pseudomallei* in light of the decreased growth of  $\Delta bpss0140$ ,  $\Delta bpss0141$  and  $\Delta bpss0142$  compared to wild type *B. pseudomallei*. The combination of both computational and experimental approaches in this study effectively improved the structural and functional identification of ABC transporters in *B. pseudomallei*. Nonetheless, the upregulation of the *bpss0140-0142* operon during *B. pseudomallei* infection and intracellular survival Chieng et al. (2012) have yet to be explained.

## ACKNOWLEDGEMENTS

This work was supported by Universiti Kebangsaan Malaysia under the Research University Grant (GUP-2020-030).

## CONFLICT OF INTEREST

The authors declare no conflict of interest.

## REFERENCES

- Adams, M.D., Wagner, L.M., Graddis, T.J., Landick, R., Antonucci, T.K., Gibson, A.L. & Oxender, D.L. 1990. Nucleotide sequence and genetic characterization reveal six essential genes for the LIV-I and LS transport systems of *Escherichia coli*. *Journal of Biological Chemistry*, 265(20): 11436-11443. [https://doi.org/10.1016/S0021-9258\(19\)38417-0](https://doi.org/10.1016/S0021-9258(19)38417-0)
- Ashdown, L.R. 1979. An improved screening technique for isolation of *Pseudomonas pseudomallei* from clinical specimens. *Pathology*, 11(2): 293-297. <https://doi.org/10.3109/00313027909061954>
- Barabote, R.D. & Saier, M.H. 2005. Comparative genomic analyses of the bacterial phosphotransferase system. *Microbiology and Molecular Biology Reviews*, 69(4): 608-634. <https://doi.org/10.1128/MMBR.69.4.608-634.2005>
- Basavanna, S., Khandavilli, S., Yuste, J., Cohen, J.M., Hosie, A.H.F., Webb, A.J., Thomas, G.H. & Brown, J.S. 2009. Screening of *Streptococcus pneumoniae* ABC transporter mutants demonstrates that LivJHMGF, a branched-chain amino acid ABC transporter, is necessary for disease pathogenesis. *Infection and Immunity*, 77(8): 3412-3423. <https://doi.org/10.1128/IAI.01543-08>
- Beis, K. 2015. Structural basis for the mechanism of ABC transporters. *Biochemical Society Transactions*, 43(5): 889-893. <https://doi.org/10.1042/BST20150047>
- Berntsson, R.P.A., Smits, S.H.J., Schmitt, L., Slotboom, D.J. & Poolman, B. 2010. A structural classification of substrate-binding proteins. *FEBS Letters*, 584(12): 2606-2617. <https://doi.org/10.1016/j.febslet.2010.04.043>
- Blum, M., Chang, H.Y., Chuguransky, S., Grego, T., Kandasamy, S., Mitchell, A., Nuka, G., Paysan-Lafosse, T., Qureshi, M., Raj, S., Richardson, L., Salazar, G.A., Williams, L., Bork, P., Bridge, A., Gough, J., Haft, D.H., Letunic, I., Marchler-Bauer, A., Mi, H., Natale, D.A., ecci, M., Orengo, C.A., Pandurangan, A.P., Rivoire, C., Sigrist, C.J.A., Sillitoe, I., Thanki, N., Thomas, P.D., Tosatto, S.C.E., Wu, C.H., Bateman, A. & Finn, R.D. 2021. The InterPro protein families and domains database: 20 years on. *Nucleic Acids Research*, 49(D1): D344-D354. <https://doi.org/10.1093/nar/gkaa977>

- Chieng, S., Carreto, L. & Nathan, S. 2012. *Burkholderia pseudomallei* transcriptional adaptation in macrophages. BMC Genomics, 13(1): 328. <https://doi.org/10.1186/1471-2164-13-328>
- Colovos, C. & Yeates, T.O. 1993. Verification of protein structures: Patterns of nonbonded atomic interactions. Protein Science, 2(9): 1511-1519. <https://doi.org/10.1002/pro.5560020916>
- Cuneo, M.J., Tian, Y., Allert, M. & Hellinga, H.W. 2008. The backbone structure of the thermophilic *Thermoanaerobacter tengcongensis* ribose binding protein is essentially identical to its mesophilic *E. coli* homolog. BMC Structural Biology, 8(1): 20. <https://doi.org/10.1186/1472-6807-8-20>
- Duangurai, T., Indrawattana, N. & Pumirat, P. 2018. *Burkholderia pseudomallei* adaptation for survival in stressful conditions. BioMed Research International, 2018(1): 1-11. <https://doi.org/10.1155/2018/3039106>
- Ford, R.C. & Beis, K. 2019. Learning the ABCs one at a time: structure and mechanism of ABC transporters. Biochemical Society Transactions, 47(1): 23-36. <https://doi.org/10.1042/BST20180147>
- Gaillard, T. 2018. Evaluation of AutoDock and AutoDock Vina on the CASF-2013 benchmark. Journal of Chemical Information and Modeling, 58(8): 1697-1706. <https://doi.org/10.1021/acs.jcim.8b00312>
- Hall, C.M., Jaramillo, S., Jimenez, R., Stone, N.E., Centner, H., Busch, J.D., Bratsch, N., Roe, C.C., Gee, J.E., Hoffmaster, A.R., Rivera-Garcia, S., Soltero, F., Ryff, K., Perez-Padilla, J., Keim, P., Sahl, J.W. & Wagner, D.M. 2019. *Burkholderia pseudomallei*, the causative agent of melioidosis, is rare but ecologically established and widely dispersed in the environment in Puerto Rico. PLoS Neglected Tropical Diseases, 13(9): e0007727. <https://doi.org/10.1371/journal.pntd.0007727>
- Harland, D.N., Dassa, E., Titball, R.W., Brown, K.A. & Atkins, H.S. 2007. ATP-binding cassette systems in *Burkholderia pseudomallei* and *Burkholderia mallei*. BMC Genomics, 8(1): 83. <https://doi.org/10.1186/1471-2164-8-83>
- Holden, M.T.G., Titball, R.W., Peacock, S.J., Cerdeno-Tarraga, A.M., Atkins, T., Crossman, L.C., Pitt, T., Churcher, C., Mungall, K., Bentley, S.D., Sebaihia, M., Thomson, N.R., Bason, N., Beacham, I.R., Brooks, K., Brown, K.A., Brown, N.F., Challis, G.L., Cherevach, I., Chillingworth, T., Cronin, A., Crosssett, B., Davis, P., DeShazer, D., Feltwell, T., Fraser, A., Hancea, Z., Hauser, H., Holroyd, S., Jagels, K., Keith, E.K., Maddison, M., Moule, S., Price, C., Quail, M.A., Rabinowitsch, E., Rutherford, K., Sanders, M., Simmonds, M., Songvilai, S., Stevens, K., Tumapa, S., Vesaratchavest, M., Whitehead, S., Yeats, C., Barrell, B.G., Oyston, P.C.F. & Parkhill, J. 2004. Genomic plasticity of the causative agent of melioidosis, *Burkholderia pseudomallei*. Proceedings of the National Academy of Sciences, 101(39): 14240-14245. <https://doi.org/10.1073/pnas.0403302101>
- Inglis, T.J.J. & Sagripanti, J.L. 2006. Environmental factors that affect the survival and persistence of *Burkholderia pseudomallei*. Applied and Environmental Microbiology, 72(11): 6865-6875. <https://doi.org/10.1128/AEM.01036-06>
- Jeckelmann, J.M. & Ermi, B. 2020. Transporters of glucose and other carbohydrates in bacteria. Pflügers Archiv - European Journal of Physiology, 472(9): 1129-1153. <https://doi.org/10.1007/s00424-020-02379-0>
- Jones, P.M. & George, A.M. 2012. Role of the D-loops in allosteric control of ATP hydrolysis in an ABC transporter. Journal of Physical Chemistry A, 116(11): 3004-3013. <https://doi.org/10.1021/jp211139s>
- Jumper, J., Evans, R., Pritzel, A., Green, T., Figurnov, M., Ronneberger, O., Tunyasuvunakool, K., Bates, R., Židek, A., Potapenko, A., Bridgland, A., Meyer, C., Kohl, S.A.A., Ballard, A.J., Cowie, A., Romera-Paredes, B., Nikolov, S., Jain, R., Adler, J., Back, T., Petersen, S., Reiman, D., Clancy, E., Zielinski, M., Steinegger, M., Pacholska, M., Berghammer, T., Bodenstein, S., Silver, D., Vinyals, O., Senior, A.W., Kavukcuoglu, K., Kohli, P. & Hassabis, D. 2021. Highly accurate protein structure prediction with AlphaFold. Nature, 596(7873): 583-589. <https://doi.org/10.1038/s41586-021-03819-2>
- Kaneko, A., Uenishi, K., Maruyama, Y., Mizuno, N., Baba, S., Kumasaka, T., Mikami, B., Murata, K. & Hashimoto, W. 2017. A solute-binding protein in the closed conformation induces ATP hydrolysis in a bacterial ATP-binding cassette transporter involved in the import of alginate. Journal of Biological Chemistry, 292(38): 15681-15690. <https://doi.org/10.1074/jbc.M117.793992>
- Kerr, I.D. 2002. Structure and association of ATP-binding cassette transporter nucleotide-binding domains. Biochimica et Biophysica Acta (BBA) - Biomembranes, 1561(1): 47-64. [https://doi.org/10.1016/S0304-4157\(01\)00008-9](https://doi.org/10.1016/S0304-4157(01)00008-9)
- Khare, D., Oldham, M.L., Orelle, C., Davidson, A.L. & Chen, J. 2009. Alternating access in maltose transporter mediated by rigid-body rotations. Molecular Cell, 33(4): 528-536. <https://doi.org/10.1016/j.molcel.2009.01.035>
- Kolich, L.R., Chang, Y.T., Coudray, N., Giacometti, S.I., MacRae, M.R., Isom, G.L., Teran, E.M., Bhabha, G. & Ekiert, D.C. 2020. Structure of MlaFB uncovers novel mechanisms of ABC transporter regulation.

- ELife, 9: 1-50. <https://doi.org/10.7554/eLife.60030>
- Krogh, A., Larsson, B., Heijne, G. & Sonnhammer, E.L.L. 2001. Predicting transmembrane protein topology with a hidden markov model: application to complete genomes. *Journal of Molecular Biology*, 305(3): 567-580. <https://doi.org/10.1006/jmbi.2000.4315>
- Laskowski, R., Rullmann, J.A., MacArthur, M., Kaptein, R. & Thornton, J. 1996. AQUA and PROCHECK-NMR: Programs for checking the quality of protein structures solved by NMR. *Journal of Biomolecular NMR*, 8(4): 477-486. <https://doi.org/10.1007/BF00228148>
- Laskowski, R.A., MacArthur, M.W., Moss, D.S. & Thornton, J.M. 1993. PROCHECK: a program to check the stereochemical quality of protein structures. *Journal of Applied Crystallography*, 26(2): 283-291. <https://doi.org/10.1107/S0021889892009944>
- Lewinson, O. & Livnat-Levanon, N. 2017. Mechanism of action of ABC importers: conservation, divergence, and physiological adaptations. *Journal of Molecular Biology*, 429(5): 606-619. <https://doi.org/10.1016/j.jmb.2017.01.010>
- Limmathurotsakul, D., Golding, N., Dance, D.A.B., Messina, J.P., Pigott, D.M., Moyes, C.L., Rolim, D.B., Bertherat, E., Day, N.P.J., Peacock, S.J. & Hay, S.I. 2016. Predicted global distribution of *Burkholderia pseudomallei* and burden of melioidosis. *Nature Microbiology*, 1(1): 15008. <https://doi.org/10.1038/nmicrobiol.2015.8>
- Linton, K.J. & Higgins, C.F. 2007. Structure and function of ABC transporters: The ATP switch provides flexible control. *Pflügers Archiv European Journal of Physiology*, 453(5): 555-567. <https://doi.org/10.1007/s00424-006-0126-x>
- Liu, F., Liang, J., Zhang, B., Gao, Y., Yang, X., Hu, T., Yang, H., Xu, W., Guddat, L.W. & Rao, Z. 2020. Structural basis of trehalose recycling by the ABC transporter LpqY-SugABC. *Science Advances*, 6(44): eabb9833. <https://doi.org/10.1126/sciadv.abb9833>
- Locher, K.P. 2016. Mechanistic diversity in ATP-binding cassette (ABC) transporters. *Nature Structural & Molecular Biology*, 23(6): 487-493. <https://doi.org/10.1038/nsmb.3216>
- López, C.M., Rholl, D.A., Trunck, L.A. & Schweizer, H.P. 2009. Versatile dual-technology system for markerless allele replacement in *Burkholderia pseudomallei*. *Applied and Environmental Microbiology*, 75(20): 6496-6503. <https://doi.org/10.1128/AEM.01669-09>
- Mandon, K., Poggi, M., Lambert, A., Østera, M. & Rudulier, D.L.E. 2001. Fructose uptake in *Sinorhizobium meliloti* is mediated by a high-affinity ATP-binding cassette transport system. *Journal of Bacteriology*, 183(16): 4709-4717. <https://doi.org/10.1128/JB.183.16.4709-4717.2001>
- Martinussen, J., Sørensen, C., Jendresen, C.B. & Kilstrup, M. 2010. Two nucleoside transporters in *Lactococcus lactis* with different substrate specificities. *Microbiology*, 156(10): 3148-3157. <https://doi.org/10.1099/mic.0.039818-0>
- Maruyama, Y., Itoh, T., Kaneko, A., Nishitani, Y., Mikami, B., Hashimoto, W. & Murata, K. 2015. Structure of a bacterial ABC transporter involved in the import of an acidic polysaccharide alginate. *Structure*, 23(9): 1643-1654. <https://doi.org/10.1016/j.str.2015.06.021>
- Neville, S.L., Sjöhamn, J., Watts, J.A., MacDermott-Opeskin, H., Fairweather, S.J., Ganio, K., Carey Hulyer, A., McGrath, A.P., Hayes, A.J., Malcolm, T.R., Davies, M.R., Nomura, N., Iwata, S., O'Mara, M.L., Maher, M.J. & McDevitt, C.A. 2021. The structural basis of bacterial manganese import. *Science Advances*, 7(32): 1-12. <https://doi.org/10.1126/sciadv.abg3980>
- Ogura, T. & Wilkinson, A.J. 2001. AAA+ superfamily ATPases: common structure--diverse function. *Genes to Cells : Devoted to Molecular & Cellular Mechanisms*, 6(7): 575-597. <https://doi.org/10.1046/j.1365-2443.2001.00447.x>
- Pettersen, E.F., Goddard, T.D., Huang, C.C., Couch, G.S., Greenblatt, D.M., Meng, E.C. & Ferrin, T.E. 2004. UCSF Chimera-A visualization system for exploratory research and analysis. *Journal of Computational Chemistry*, 25(13): 1605-1612. <https://doi.org/10.1002/jcc.20084>
- Scheepers, G.H., Lycklama a Nijeholt, J.A. & Poolman, B. 2016. An updated structural classification of substrate-binding proteins. *FEBS Letters*, 590(23): 4393-4401. <https://doi.org/10.1002/1873-3468.12445>
- Snider, J., Thibault, G. & Houry, W.A. 2008. The AAA+ superfamily of functionally diverse proteins. *Genome Biology*, 9(4): 216. <https://doi.org/10.1186/gb-2008-9-4-216>
- Taga, M.E., Semmelhack, J.L. & Bassler, B.L. 2008. The LuxS-dependent autoinducer AI-2 controls the expression of an ABC transporter that functions in AI-2 uptake in *Salmonella typhimurium*. *Molecular Microbiology*, 42(3): 777-793. <https://doi.org/10.1046/j.1365-2958.2001.02669.x>
- Tanaka, K.J., Song, S., Mason, K. & Pinkett, H.W. 2018. Selective substrate uptake: The role of ATP-binding cassette (ABC) importers in pathogenesis. *Biochimica et Biophysica Acta (BBA) - Biomembranes*, 1860(4): 868-877. <https://doi.org/10.1016/j.bbamem.2017.08.011>
- Thomas, C. & Tampé, R. 2020. Structural and mechanistic principles of ABC transporters. *Annual Review*

- of Biochemistry, 89(1): 605-636. <https://doi.org/10.1146/annurev-biochem-011520-105201>
- Trott, O. & Olson, A.J. 2010. AutoDock Vina: improving the speed and accuracy of docking with a new scoring function, efficient optimization, and multithreading. *Journal of Computational Chemistry*, 31(2): 455-461. <https://doi.org/10.1002/jcc.21334>
- Tsai, H.H.G., Tsai, C.J., Ma, B. & Nussinov, R. 2009. In silico protein design by combinatorial assembly of protein building blocks. *Protein Science*, 13(10): 2753-2765. <https://doi.org/10.1110/ps.04774004>
- Vanaporn, M., Sarkar-Tyson, M., Kovacs-Simon, A., Ireland, P.M., Pumirat, P., Korbsrisate, S., Titball, R.W. & Butt, A. 2017. Trehalase plays a role in macrophage colonization and virulence of *Burkholderia pseudomallei* in insect and mammalian hosts. *Virulence*, 8(1): 30-40. <https://doi.org/10.1080/21505594.2016.1199316>
- Verdon, G., Albers, S.V., Dijkstra, B.W., Driessen, A.J.M. & Thunnissen, A.M.W.H. 2003. Crystal structures of the ATPase subunit of the glucose ABC transporter from *Sulfolobus solfataricus*: nucleotide-free and nucleotide-bound conformations. *Journal of Molecular Biology*, 330(2): 343-358. [https://doi.org/10.1016/S0022-2836\(03\)00575-8](https://doi.org/10.1016/S0022-2836(03)00575-8)
- Wagner, M., Shen, L., Albersmeier, A., Kolk, N., Kim, S., Cha, J., Bräsen, C., Kalinowski, J., Siebers, B. & Albers, S.V. 2018. *Sulfolobus acidocaldarius* transports pentoses via a carbohydrate uptake transporter 2 (CUT2)-type ABC transporter and metabolizes them through the aldolase-independent Weimberg pathway. *Applied and Environmental Microbiology*, 84(3): 1-19. <https://doi.org/10.1128/AEM.01273-17>
- Wei, X., Guo, Y., Shao, C., Sun, Z., Zhurina, D., Liu, D., Liu, W., Zou, D., Jiang, Z., Wang, X., Zhao, J., Shang, W., Li, X., Liao, X., Huang, L., Riedel, C.U. & Yuan, J. 2012. Fructose uptake in *Bifidobacterium longum* NCC2705 is mediated by an ATP-binding cassette transporter. *Journal of Biological Chemistry*, 287(1): 357-367. <https://doi.org/10.1074/jbc.M111.266213>
- Wong, R.R., Kong, C., Lee, S.H. & Nathan, S. 2016. Detection of *Burkholderia pseudomallei* toxin-mediated inhibition of protein synthesis using a *Caenorhabditis elegans* ugt-29 biosensor. *Scientific Reports*, 6(1): 27475. <https://doi.org/10.1038/srep27475>
- Woodson, K. & Devine, K.M. 1994. Analysis of a ribose transport operon from *Bacillus subtilis*. *Microbiology*, 140(8): 1829-1838. <https://doi.org/10.1099/13500872-140-8-1829>
- Wu, Q., Peng, Z., Zhang, Y. & Yang, J. 2018. COACH-D: improved protein-ligand binding sites prediction with refined ligand-binding poses through molecular docking. *Nucleic Acids Research*, 46(W1): W438-W442. <https://doi.org/10.1093/nar/gky439>
- Xavier, K.B. & Bassler, B.L. 2005. Regulation of uptake and processing of the quorum-sensing autoinducer AI-2 in *Escherichia coli*. *Journal of Bacteriology*, 187(1): 238-248. <https://doi.org/10.1128/JB.187.1.238-248.2005>
- Yang, J., Roy, A. & Zhang, Y. 2013. Protein-ligand binding site recognition using complementary binding-specific substructure comparison and sequence profile alignment. *Bioinformatics*, 29(20): 2588-2595. <https://doi.org/10.1093/bioinformatics/btt447>
- Yu, N.Y., Wagner, J.R., Laird, M.R., Melli, G., Rey, S., Lo, R., Dao, P., Sahinalp, S.C., Ester, M., Foster, L.J. & Brinkman, F.S.L. 2010. PSORTb 3.0: improved protein subcellular localization prediction with refined localization subcategories and predictive capabilities for all prokaryotes. *Bioinformatics*, 26(13): 1608-1615. <https://doi.org/10.1093/bioinformatics/btq249>
- Zhou, C., Zheng, Y. & Zhou, Y. 2004. Structure prediction of membrane proteins. *Genomics, Proteomics & Bioinformatics*, 2(1): 1-5. [https://doi.org/10.1016/S1672-0229\(04\)02001-7](https://doi.org/10.1016/S1672-0229(04)02001-7)
- Zulkefli, N.J., Teh, C.S.J., Mariappan, V., Ngoi, S.T., Vadivelu, J., Ponnampalavanar, S., Chai, L.C., Chong, C.W., Yap, I.K.S. & Vellasamy, K.M. 2021. Genomic comparison and phenotypic profiling of small colony variants of *Burkholderia pseudomallei*. *PLoS ONE*, 16(12): e0261382. <https://doi.org/10.1371/journal.pone.0261382>

